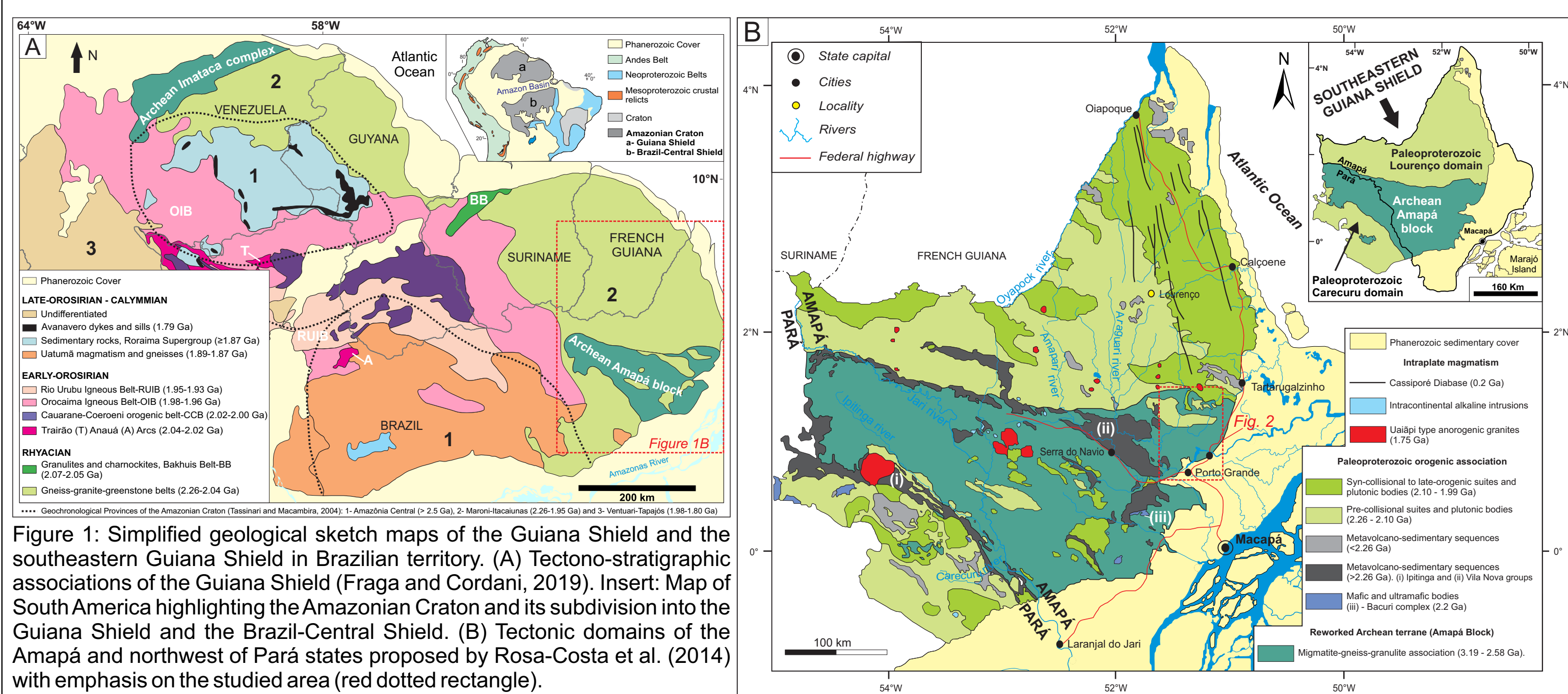


INTRODUCTION

The late Rhyacian high-grade metamorphic complex (Tartarugal Grande Complex - TGC; Fig. 1) is located at the transition between the Rhyacian Lourenço domain and the Archean Amapá block, in the central eastern region of the state of Amapá, Brazil, southeastern Guiana Shield (Rosa-Costa et al., 2006, 2014; Gorayeb et al., 2021). The Amapá Block, to the south, is a large Archean continental landmass roughly oriented in a WNW-ESE direction. It consists mainly of a high-grade metamorphic granulitic-migmatitic-gneiss complex of Meso- to Neoproterozoic age (3.19-2.60 Ga), strongly reworked during the Transamazonian orogeny, responsible for its deformation, metamorphism and granitic magmatism. The Lourenço Domain, to the north, is constituted by a Rhyacian lithological association of granitoid-greenstones, with dominant granitoids and orthogneisses and restricted metavolcanosedimentary sequences metamorphosed in the greenschist to amphibolite facies, locally granulite (Rosa-Costa et al., 2006, Milhomem Neto and Lafon, 2019). This granitoid-greenstone association formed in a long-lived continental magmatic arc setting (~2.26-2.12 Ga), which evolved to a collisional setting with the amalgamation of the Amapá Block and the Lourenço Domain at 2.11–2.08 Ga (Rosa-Costa et al., 2014; Milhomem Neto & Lafon, 2020; Vianna et al., 2020).



The TGC rocks outcrop in the beds of the Tartarugal Grande and Falsino Rivers, on the margins of the BR-156 highway (Macapá-Oyapock) and nearby roads (Fig. 2). The TGC encompasses an association of high-grade metamorphic rocks composed by dominant felsic granulites and aluminous leucogneisses, besides of rare mafic granulites and amphibolites that occur as tabular bodies or lenses of metrical dimensions intruded in the felsic granulite and leucogneiss protoliths, before metamorphism. It also includes some charnockite and granite bodies with preserved magmatic structures. Both granulites and gneisses were affected by thrust and transcurrent shear zones along a NW-SE trend. Quartz-feldspathic neosomes, with or without orthopyroxene and garnet-rich neosomes occur in the felsic granulites and the leucogneisses, respectively, as a product of anatexis. The peak of granulite metamorphism was estimated by Gorayeb et al. (2021) at 800 ± 20 °C (temperature) and 6-7 kbar (pressure). Retro-metamorphism and cooling during exhumation to higher crustal levels was also evidenced. A geochronological data set indicates that the TGC includes rocks formed during the Rhyacian and the Neoproterozoic and metamorphosed during a late Transamazonian granulite episode (Table 1). In this work we present a new set of LA-ICP-MS U-Pb ages for monazites from two leucogneisses, a neosome derived from a migmatitic leucogneiss and for zircons from an amphibolite (Fig. 3) from the TGC to better constrain the timing of the high-grade metamorphism in this part of the southeast Guiana Shield.

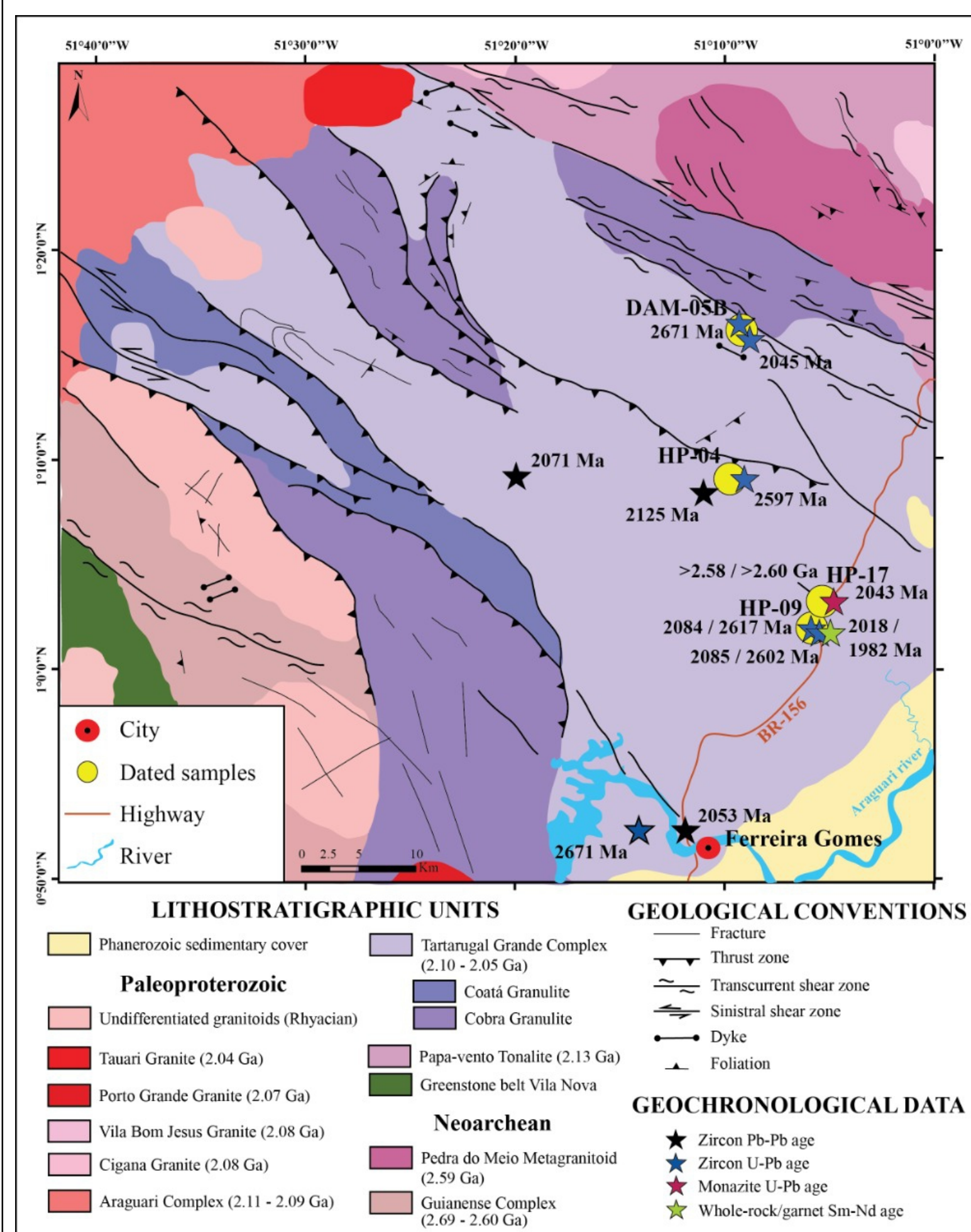


Table 1- Summary of geochronological data for granulites and gneisses from the Tartarugal Grande Complex

Rock Type	Age	Method	Interpretation	Ref.
Garnet-biotite gneiss	>2.58 Ga	Pb-evaporation zircon (TIMS)	Inheritance	1
Charnokitic granulite	>2.60 Ga	Pb-evaporation zircon (TIMS)	Minimum age (protolith)	1
Charnokitic granulite	2053 ± 1 Ma	Pb-evaporation zircon (TIMS)	Crystallization of protolith	1
Charnokitic granulite	2078 ± 4 Ma	Pb-evaporation zircon (TIMS)	Crystallization of protolith	2
Enderbitic granulite	2100 ± 4 Ma	Pb-evaporation zircon (TIMS)	Crystallization of protolith	2
Enderbitic granulite	2092 ± 7 Ma	Pb-evaporation zircon (TIMS)	Crystallization of protolith	2
Charnokitic granulite	2597 ± 55 Ma	U-Pb zircon (LA-ICP-MS)	Crystallization of protolith	2
Charnokitic granulite	2671 ± 15 Ma	U-Pb zircon (LA-ICP-MS)	Crystallization of protolith	2
Felsic granulite	2623 ± 13 Ma	U-Pb zircon (SHRIMP)	Crystallization of protolith	3
Felsic granulite	2.67–2.48 Ga	U-Pb zircon (LA-ICP-MS)	Archean inheritance	4
Felsic granulite	2043 ± 8 Ma	U-Pb monazite (LA-ICP-MS)	Metamorphic age	4
Felsic granulite	1966 ± 13 Ma	⁴⁰ Ar- ³⁹ Ar biotite	Metamorphic cooling age	4
Felsic granulite	2037 ± 8 to 2017 ± 12 Ma	Sm-Nd whole rock-garnet (TIMS)	Metamorphic age	5
Garnet-biotite gneiss	2018 ± 2 to 1982 ± 3 Ma	Sm-Nd whole rock-garnet (TIMS)	Metamorphic age	5
Enderbitic granulite	2084 ± 8 Ma	U-Pb zircon (LA-ICP-MS)	Crystallization of protolith	6
Charnokitic granulite	2045 ± 14 Ma	U-Pb zircon (LA-ICP-MS)	Metamorphic age	6

Figure 2: Geological map of the TGC occurrence region. Adapted from Rosa-Costa et al. (2014) and Barbosa & Chaves (2015).

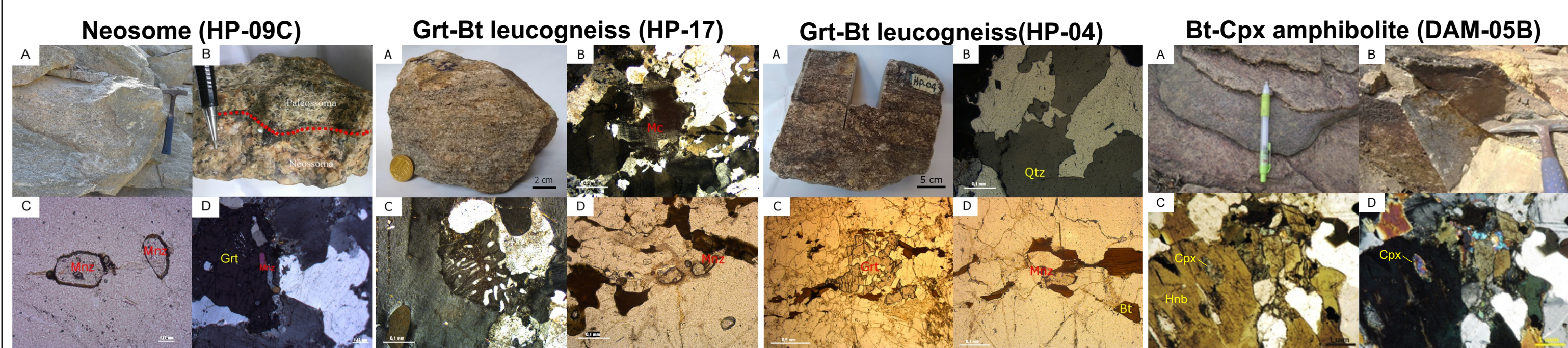


Figure 3: Petrographic aspects of the samples investigated in this study. HP-09C: A) Outcrop in a quarry, B) Hand sample highlighting the neosome of a migmatitic leucogneiss, C) and D) monazite crystals included in feldspar and garnet, respectively. HP-17: A) hand sample of leucogneiss, B) C) and D) photomicrographs highlighting the main and accessory mineralogy (microcline, microcline plagioclase and monazites). HP-04: A) Leucogneiss hand sample, B) C) and D) photomicrographs highlighting the main and accessory mineralogy with quartz, garnet, biotite and monazite. DAM-05B: A) and B) amphibolite beds intercalated in felsic granulite, C) and D) crystals of diopside associated with hornblende.

SAMPLING AND ANALYTICAL METHODS

Samples from previous studies (Paiva, 2016; acronym HP) and from the collection of the Research Group in Isotope Geology at UFPA (Acronym DAM) were used. Four samples including leucogneisses and one amphibolite from the eastern portion of the TGC were selected. Separation and concentration procedures for monazite and zircon, mounts preparation and scanning electron microscopy (SEM) were performed using at the laboratory facilities of the UFPA Geoscience Institute. LA-MC-ICP-MS monazite U-Pb analyses were carried out using a multi-collector Neptune Thermo Finnigan mass spectrometer coupled with a Nd:YAG LSX-213 G2 CETAC laser microprobe at the Pará-Iso. The analytical conditions, instrumental corrections, raw data reduction and age calculation are described in Ferreira (2022). LA-MC-ICP-MS zircon U-Pb dating of the amphibolite sample was carried at the Geochronological Laboratory of the Brasília University, using similar equipment to those of the Pará-Iso and following Buhh et al. (2009).

RESULTS

The samples of this study were petrographically classified as a garnet-biotite leucogneiss of monzogranitic composition (Sample HP-04), a garnet-biotite leucogneiss of syenogranitic composition (Sample HP-17), a neosome derived from a migmatitic leucogneiss (HP-09C) associated with felsic granulites and one biotite-clinopyroxene amphibolite which occurs as centimeter wide lenses in felsic granulites (sample DAM-05B). Metamorphic conditions are similar to those described by Gorayeb et al. (2021). U-Pb ages obtained on monazite and zircon grains are listed in Table 2 and presented in the diagrams of figure 4.

Table 2- Summary of the LA-ICP-MS U-Pb ages obtained in this work for the samples of the Tartarugal Grande Complex

Lithology	Sample	U-Pb assigned age (Ma)	Statistical parameters	Mineral
Neosome of migmatitic leucogneiss	HP-09C	2056 ± 5*	2σ; n = 30; MSWD = 0.31	Monazite
Garnet-biotite leucogneiss	HP-17	2058 ± 19**	2σ; n = 51; MSWD = 0.64	Monazite
Garnet-biotite leucogneiss	HP-04	2096 ± 16 to 2056 ± 16***	2σ; n = 27	Monazite
Biotite-clinopyroxene amphibolite	DAM-05B	2069 ± 11*	2σ; n = 6; MSWD = 0.47	Zircon

*U-Pb Concordia Age, **Upper intercept age, ***²⁰⁷Pb/²⁰⁶Pb range dates.

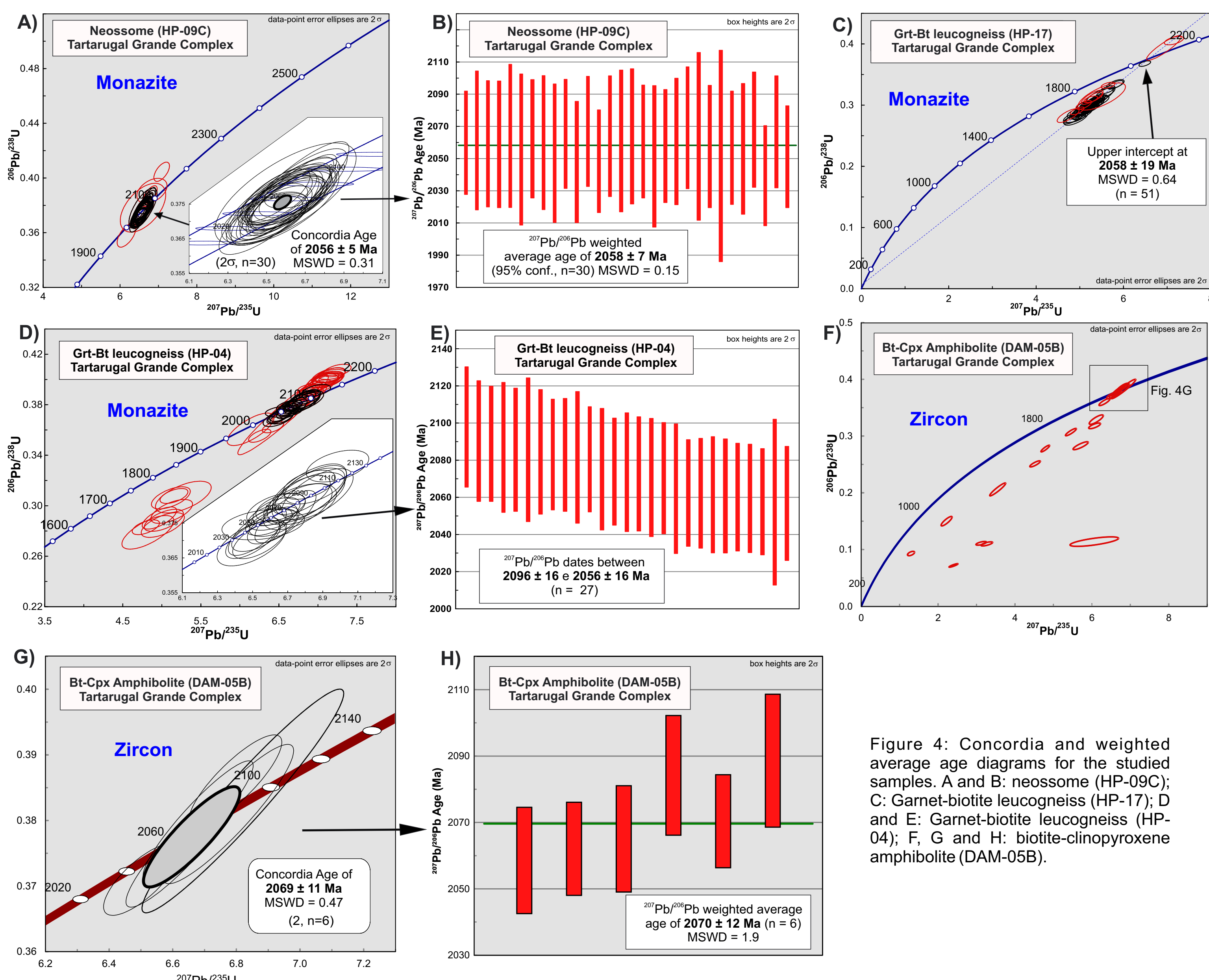


Figure 4: Concordia and weighted average age diagrams for the studied samples. A and B: neosome (HP-09C); C: Garnet-biotite leucogneiss (HP-17); D and E: Garnet-biotite leucogneiss (HP-04); F, G and H: biotite-clinopyroxene amphibolite (DAM-05B).

TIMING CONSTRAINTS ON THE HIGH-GRADE METAMORPHISM OF THE TGC

The new U-Pb results on monazite and zircon and the previous geochronological data on rocks from the TGC and neighboring magmatic units indicate a magmatic-metamorphic event at the end of the Rhyacian and beginning of the Orosirian in the central region of Amapá marked by intense magmatism between ~2.10 and 2.08 Ga. This magmatic episode triggered regional warming and was followed by a high temperature, intermediate pressure metamorphic event that affected both Archean ortho and paraderived rocks and Rhyacian granulites. This episode, with a metamorphism peak around 2.06-2.04 Ga, produced granulite rocks, local migmatization and the intrusion of charnockitic plutons. Metamorphic cooling occurred between ~2.04 and ~1.98 Ga until reaching a temperature below 300°C around 1.97 Ga (⁴⁰Ar-³⁹Ar biotite metamorphic cooling age; Enjoly, 2008). The high-grade metamorphism in central Amapá (2.06-2.04 Ga) is coeval with the UHT metamorphism of the Bakhuish granulitic belt in Suriname (2.09-2.03 Ga; De Roeover et al., 2003, 2019, Klaver et al., 2015, 2016), however, this does not imply that were generated by the same metamorphic processes. The model of mantle upwelling in a zone of maximum crustal thinning associated with vertical tectonics proposal by Delor et al. (2003) seems more consistent to explain the formation of the TGC.

MAJOR EVENTS IN THE EVOLUTION OF THE TARTARUGAL GRANDE GRANULITIC COMPLEX

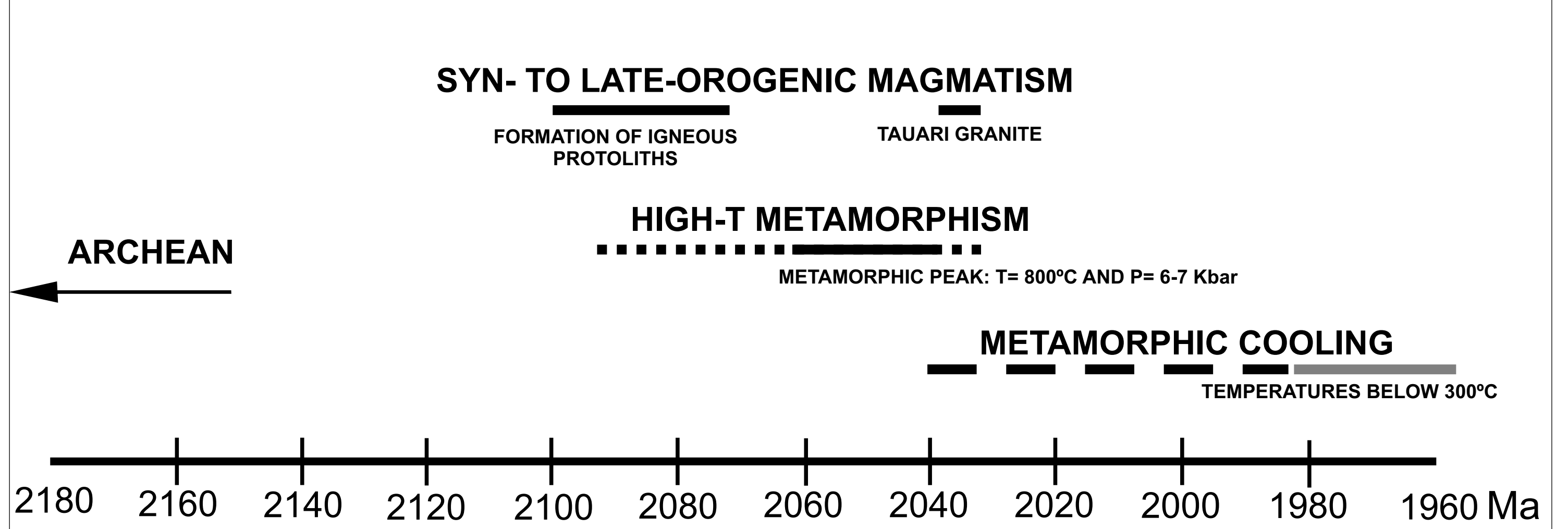


Figure 5: Synthesis of the chronology of magmatic and metamorphic events of the Tartarugal Grande granulitic complex.

ACKNOWLEDGMENTS

This work was supported through the P1061B AMIRA PROJECT "South American Exploration Initiative Stage 2 (SAXI 2)-module 7A" and by the Conselho Nacional de Desenvolvimento Científico e Tecnológico (CNPq)/UNIVERSAL PROJECT (Grant No. 423625/2018-7). This contribution is part of the Master's thesis of the third author (D.P.A.F.).

REFERENCES

Avelar, V.G., 2002. Geochronologia Pb-Pb em zircão e Sm-Nd em rocha total da porção centro-norte do Estado do Amapá-Escala: Implicações para a evolução geodinâmica do setor oriental do Escudo das Guianas (Ph.D. Dissertation), Federal University of Pará-Brazil, 213 p (in Portuguese).
Barbosa, J.P.O., Chaves, C.L., 2015. Geologia e Recursos Minerais da Folha Macapá - NA.22-YD, Estado do Amapá, Escala 1:250.000. CPRM - Geological Survey of Brazil, Belém, p. 116p.
Bélou, B., Pimentel, M.M., Mattaini, M., Dantas, E.L., 2009. High spatial resolution analysis of Pb and U isotopes for geochronology by laser ablation multi-collector inductively coupled plasma spectrometry (LA-MC-ICP-MS). An. Acad. Bras. Cienc. 81: 99-114.
Delor, C., Lahondère, D., Egal, E., Lafon, J.M., Cocherie, A., Guerot, C., Rossi, P., Truffert, C., Theveniaut, H., Phillips, D., Avelar, V.G., 2003. Transamazonian Crustal Growth and Reworking as Revealed by the 1500-000 - Scale Geological Map of French Guiana, second ed., 2-3-4. Géologie de la France - Special Guiana Shield. BRGM-SGFR. Editor, pp. 5-58 De Roeover, E.W.F., Lafon, J.M., Delor, C., Cocherie, A., Rossi, P., Guerot, C., Potrel, A., 2003. The Bakhuish ultrahigh-temperature granulite belt (Suriname): A petrological and geochronological evidence for a counterclockwise P-T path at 2.07 and 2.02 Ga. Géologie de la France 2: 175-206.
De Roeover, E.W.F., Beunk, F.F., Yik, Groot, K., Klaver, M., Nanne, J.A.M., Steeg, W., Thijssen, A.C.D., Lunck, B., Vos, H., Davies, G.R., Browner, F.M., 2019. The Bakhuish granulite belt in W Suriname, its development and exhumation. In: 11th Guiana geol conference: the tectonics and resource potential of NE-south America, Paramaribo, Guayana Francesa. Dineri Suriname Meded. 29:53-58.
Fraga, L.M., Cordani, U., 2019. Early Orosirian tectonic evolution of the Central Guiana Shield: insights from new U-Pb SHRIMP data. In: SAXI - XI Inter Guiana Geological Conference, Paramaribo, Suriname. Extended abstract, pp. 59-62.
Gorayeb, P.S., Paiva, M.P.S., Lafon, J.M., Rosa-Costa, L.T., Dantas, E.L., 2021. Petrological and geochronological evolution of the Tartarugal Grande Granulitic Complex - Northeastern Amazonian Craton. Journal of South American Earth Sciences 112: 103549.
Klaver, M., Roeover, E.W.F., Nanne, J.A.M., Mason, P.R., Davies, G.R., 2015. Charnokites and UHT metamorphism in the Bakhuish Granulite Belt, western Suriname: evidence for two separate UHT events. Precambrian Research 262:1-19.
Klaver, M., Roeover, E.W.F., Thijssen, A.C.D., Bleeker, W., Soderlund, U., Chamberlain, K., Ernst, R., Berndt, J., Zeh, A., 2016. Mafic magmatism in the Bakhuish Granulite Belt (western Suriname): relationship with charnockite magmatism and UHT metamorphism. GFF 138:203-216.
Milhomem Neto, J.M., Lafon, J.M., 2019. Zircon U-Pb and Lu-Hf isotope constraints on Archean crustal evolution in Southeastern Guiana Shield. Geoscience Frontiers 10: 1477-1506.
Milhomem Neto, J.M., Lafon, J.M., 2020. Crustal growth and reworking of Archean crust within the Rhyacian domains of the southeastern Guiana Shield, Brazil: Evidence from zircon U-Pb-Hf and whole-rock Sm-Nd geochronology. Journal of South American Earth Sciences 103: 102740.
Oliveira, E.C., Lafon, J.M., Gioia, S.M.C.L., Pimentel, M.M., 2008. Datasão Sm-Nd em rocha total e granulada do metamorfismo granulítico da região de Tartarugal Grande, Amapá, Central. Revista Brasileira de Geociências 38: 116-129 (in Portuguese).
Paiva, H.S., 2016. Caracterização petrográfica, geoquímica e geocronológica U-Pb em docha total e granulada do metamorfismo granulítico do complexo Tartarugal Grande, Sudeste do Estado das Guianas, Amapá (Master's Thesis), Federal University of Pará-Brazil, 89p (in Portuguese).
Rosa-Costa, L.T., Lafon, J.M., Delor, C., 2006. Zircon geochronology and Sm-Nd isotope study: further constraints for the geodynamical evolution during Archean and Paleoproterozoic in the Southeast of Guiana Shield, north of Brazil. Gondwana Research 10: 277-300.
Rosa-Costa, L.T., Chaves, C.L., Klein, E.L., 2014. Geologia e recursos minerais da Folha Rio Araguaia e NA.22-YB, Estado do Amapá, Escala 1:250.000. CPRM, Belém, 159p (in Portuguese).
Tassinari, C.G. et al., 2004. The Imataca Complex, NW Amazonian Craton, Venezuela. Episodes, 27: 3-12.
Vianna, S.Q., Lafon, J.M., Milhomem Neto, J.M., Silva, D.P.B., Barros, C.E.M., 2020. U-Pb geochronology, Nd-Hf isotopes, and geochemistry of rhyacian granulites from the Paleoproterozoic Lourenço domain (Brazil), southeastern Guiana shield. Journal of South American Earth Sciences 106: 102937.